



# Wastewater injection, aquifer biogeochemical reactions, and resultant groundwater N fluxes to coastal waters: Kā'anapali, Maui, Hawai'i



Joseph K. Fackrell<sup>a,\*</sup>, Craig R. Glenn<sup>a,\*</sup>, Brian N. Popp<sup>a</sup>, Robert B. Whittier<sup>b</sup>, Henrietta Dulai<sup>a</sup>

<sup>a</sup> University of Hawai'i at Mānoa, Department of Geology and Geophysics, 1680 East West Road, POST 701, Honolulu, HI 96822, USA

<sup>b</sup> Hawai'i Department of Health, Safe Drinking Water Branch, 919 Ala Moana Boulevard, Honolulu, HI 96814, USA

## ARTICLE INFO

### Article history:

Received 25 August 2015

Received in revised form 7 June 2016

Accepted 12 June 2016

Available online 20 June 2016

### Keywords:

Wastewater treatment

Underground injection

Nitrogen cycle

Denitrification

Anammox

Submarine groundwater discharge

## ABSTRACT

We utilize N and C species concentration data along with  $\delta^{15}\text{N}$  values of  $\text{NO}_3^-$  and  $\delta^{13}\text{C}$  values of dissolved inorganic C to evaluate the stoichiometry of biogeochemical reactions (mineralization, nitrification, anammox, and denitrification) occurring within a subsurface wastewater plume that originates as treated wastewater injection and enters the coastal waters of Maui as submarine groundwater discharge. Additionally, we compare wastewater effluent time-series data, injection rates, and treatment history with submarine spring discharge time-series data. We find that heterotrophic denitrification is the primary mechanism of N loss within the groundwater plume and that chlorination for pathogen disinfection suppresses microbial activity in the aquifer responsible for N loss, resulting in increased coastal ocean N loading. Replacement of chlorination with UV disinfection may restore biogeochemical reactions responsible for N loss within the aquifer and return N-attenuating conditions in the effluent plume, reducing N loading to coastal waters.

© 2016 Elsevier Ltd. All rights reserved.

## 1. Introduction

The introduction of excess anthropogenic N to coastal waters from the terrestrial environment is recognized as a major driver of coastal ocean eutrophication, whose effects include mass algae blooms, the development of hypoxic “dead zones,” and degradation of original habitat (e.g. Paerl, 1997; Scavia and Bricker, 2006; Bricker et al., 2007; Howarth and Marino, 2006). Coral reef ecosystems are in decline worldwide as a result of a variety of environmental stressors (Bruno and Selig, 2007; Wilkinson, 2008) and, while the relative contribution of N pollution to this decline with respect to other stressors such as global warming and ocean acidification can be debated (Szmant, 2002), there is clear evidence that corals can be susceptible to damage from N-fuelled algae blooms, which can smother reefs and block light from reaching coral's symbiotic algae (e.g. Smith et al., 1981; Paytan et al., 2006; DeGeorges et al., 2010). Common sources of N to coastal waters include fertilizer and municipal and industrial wastewater, which can be transported to the ocean via surface runoff and through the subsurface as submarine groundwater discharge (SGD).

SGD is commonly enriched in nutrients relative to ocean surface waters and can transport the majority of land-derived N and other nutrients to coastal waters, even in areas where significant surface water

discharge occurs (Burnett et al., 2003; Garrison et al., 2003; Moore, 2006; Kwon et al., 2014). SGD consists of both fresh water and recirculated seawater and typically enters coastal waters via a brackish zone of subsurface mixing termed the subterranean estuary (Moore, 1999). The subterranean estuary is a hydraulically dynamic and geochemically reactive zone in which biogeochemical transformations involving N and other dissolved species occur (e.g. Slomp and Van Cappellen, 2004; Kroeger and Charette, 2008; Spiteri et al., 2008). Because N transformations in the subterranean estuary can govern the spatial and temporal changes in the rate of N species delivery to coastal waters, understanding the nature and extent of these reactions is necessary to characterizing N flux from this complex zone.

$\text{NO}_3^-$  reduction, the bacterially mediated stepwise transformation of aqueous  $\text{NO}_3^-$  to  $\text{N}_2$  gas, is the primary means of bioactive N loss in groundwater (Kendall, 1998). The reaction typically requires suboxic conditions, the presence of an electron donor, and a population of denitrifying bacteria (Kehew, 2000). Factors that affect these requirements have the potential to disrupt the  $\text{NO}_3^-$  reduction reaction.  $\text{NO}_3^-$   $\delta^{15}\text{N}$  values can be diagnostic of  $\text{NO}_3^-$  source provenance and various transformative processes in the N cycle (e.g. Kendall, 1998; Granger et al., 2008). N isotope values have been used in groundwater studies (e.g. Aravena and Robertson, 1998) and marine studies (e.g. Sigman et al., 2005) to trace the sources and evolution of  $\text{NO}_3^-$ . In this study we use  $\text{NO}_3^-$   $\delta^{15}\text{N}$  values and  $\text{NO}_3^-$  concentrations as indicators of  $\text{NO}_3^-$  reduction. The microorganisms responsible for denitrification preferentially reduce  $^{14}\text{NO}_3^-$  into  $\text{N}_2$ , leaving the remaining  $\text{NO}_3^-$  relatively enriched in  $^{15}\text{N}$  (Kendall, 1998).

\* Corresponding authors.

E-mail addresses: [fackrell@hawaii.edu](mailto:fackrell@hawaii.edu) (J.K. Fackrell), [glenn@soest.hawaii.edu](mailto:glenn@soest.hawaii.edu) (C.R. Glenn).

Dissolved organic C (DOC) is a key species in facilitating  $\text{NO}_3^-$  reduction in groundwater. DOC is a source of sustenance for heterotrophic microorganisms that preferentially utilize available dissolved  $\text{O}_2$  (DO) as an electron acceptor in aerobic respiration due to its high energy yield. When DOC remains in excess as DO concentrations become suboxic, capable microorganisms shift to anaerobic respiration using available  $\text{NO}_3^-$  as an electron acceptor (reducing  $\text{NO}_3^-$  to  $\text{N}_2$  gas) to facilitate the oxidation of organic C to dissolved inorganic C (DIC) (Froelich et al., 1979; Stumm and Morgan, 1996; Kehew, 2000). Species such as  $\text{Fe}^{2+}$  may also be oxidized in  $\text{NO}_3^-$  reduction in subterranean estuaries with DOC poor conditions (Kroeger and Charette, 2008).  $\delta^{13}\text{C}$  values of DIC, when considered in conjunction with DOC and DIC concentrations, can be a useful tool in identifying DIC produced by the  $\text{NO}_3^-$  reduction (Aravena and Robertson, 1998) as well as evaluating  $\text{NO}_3^-$  reduction stoichiometry and the potential for the participation of electron donors other than DOC in the reaction.

The purpose of this study is to evaluate the mechanisms controlling the N flux from SGD from submarine springs offshore of Kahekili Beach Park on the island of Maui, Hawai'i. These submarine springs have been demonstrated to discharge treated wastewater effluent injected underground at Lahaina Wastewater Reclamation Facility (LWRF), approximately 0.5 km inland (Glenn et al., 2012, 2013). In this work we utilize LWRF effluent and submarine spring N species data along with  $\delta^{15}\text{N}$  values of dissolved  $\text{NO}_3^-$ , C species concentrations, and  $\delta^{13}\text{C}$  values of DIC to evaluate the stoichiometry of biogeochemical reactions occurring within the subsurface effluent plume. Additionally, we consider as a whole LWRF effluent and submarine spring N species data collected over the last several years to examine how changes in effluent injection rate as well as treatment and disinfection practices control the temporal variability in the extent of N species transformation and loss occurring within the effluent plume and, consequently, the variability of N flux to coastal waters from this source.

## 2. Study area/background

### 2.1. Study area description

The Kā'anapali region (Fig. 1) is located on the relatively dry, lightly dissected leeward portion of the West Maui volcano (1.2–1.6 Ma). The geology of this area is dominated by the shield building Wailuku Volcanic series overlain by a thin veneer of later stage Honolua Volcanic series lavas in the northern portion of the study area. The rejuvenated stage Lahaina Volcanic series (age unknown) occurs as vents at Pu'u Keka'a (Black Rock) and further south near the town of Lahaina (Stearns and Macdonald, 1942). A narrow band of coastal alluvium, consisting of both terrestrial and marine sediments, fronts the coast at most locations in the study area. The area's groundwater exists primarily as an unconfined basal lens with low hydraulic gradients due to the high hydraulic conductivity of the basaltic aquifer (Stearns and Macdonald, 1942; Gingerich and Engott, 2012). Although locally confining conditions may exist in the coastal alluvium, they are not widespread enough to create a discernible effect on the larger scale water table levels of the basal lens (Souza, 1981). Dike confined high-level groundwater exists in the far upland portion of the study area near the summit of the West Maui volcano, where the area's rainfall and groundwater recharge rates are highest (Engott and Vana, 2007).

The marine portion of the study area is located within the Kahekili Herbivore Fisheries Management area, established in July 2009 to restore a healthy population of algae grazing fishes to the region. Though a fringing reef is present near the shore, the seafloor slopes rapidly to depths over 30 m just 500 m offshore. Coral cover at depths of 3 m and 7 m have declined from ca. 50–60% in 1994 to ca. 20–30% in 2005, a reduction more dramatic than the average observed decline during this period for Maui study sites as a whole. Additionally, macroalgae cover at 3 m increased from near 0% to over 20% for the same period (Williams and Sparks, 2008).

Land use in the Kā'anapali area was long dominated by intensive sugar cane cultivation south of Honokōwai stream and pineapple cultivation north of Honokōwai stream, but recently both industries have declined, with sugar cane and pineapple cultivation ceasing entirely in 1999 and 2009, respectively. The area now consists primarily of resort, golf course, and light commercial development along the coastline with former agricultural fields on lower slopes (to about 400 m elevation) and state forest reserves on the slopes above. Wastewater is processed at the LWRF, located approximately 0.5 km inland from Kahekili Beach, and disposed of via 4 vertical on-site injection wells drilled to roughly 60 m below sea level. This facility has undergone several expansions and treatment upgrades since its inception in 1975. The capacity of LWRF was increased from 3.2 to 6.7 MGD by construction of an additional plant onsite in 1985 (Tetra Tech, Inc., 1993), and in 1995 biological nutrient removal and partial UV disinfection capabilities were instituted to further treat wastewater before injection (County of Maui Wastewater Reclamation Division, personal communication). LWRF effluent was disinfected using chlorination under an EPA mandate from October 2011 to May 2014, when full UV disinfection capabilities were certified. The facility is currently capable of treating effluent to irrigation (R-1) quality using UV disinfection and had mean injection and reuse flows of 3.3 and 0.9 MGD, respectively, in the period from January 2011 to July 2014.

### 2.2. Background

The occurrence of periodic large scale algal blooms in the Kā'anapali area beginning in the 1980s has raised concerns regarding the impacts of land use practices on the coastal environment. Several studies, including an inconclusive dye tracer injection test at the LWRF injection wells (Tetra Tech, Inc., 1994), were conducted to address these concerns (e.g. Tetra Tech, Inc., 1993; Dollar and Andrews, 1997). Various modeling approaches combined with in situ measurements were used to assess the contributions of land use activities to coastal nutrient delivery from both ground and surface waters (Tetra Tech, Inc., 1993; Soicher, 1996; Soicher and Peterson, 1997). Dollar and Andrews (1997) and Laws et al. (2004) examined the area's coastal water quality by comparing nutrient concentrations across various locations. Dollar and Andrews (1997) also measured the N isotopic composition of algal tissue in an attempt to determine the contribution of terrestrially-derived N. More recently, analysis of nutrient species, and stable isotopic compositions of water and dissolved  $\text{NO}_3^-$  (Hunt and Rosa, 2009), N isotopic composition in algal tissue (Dailer et al., 2010, 2012), and analysis of trace metals, radon, nutrient species, and subsurface electrical resistivity (Swarzenski et al., 2012) were used to ascertain pathways of nutrient delivery to coastal waters. These studies found that the coastal ocean along Kahekili Beach Park roughly 1 km southwest of the LWRF injection wells was characterized by elevated  $\delta^{15}\text{N}$  values in algal tissue, higher temperatures, and lower water pH values relative to adjacent areas. These findings were interpreted as evidence for injected effluent discharging into coastal waters along this coastline. The detection of wastewater indicator compounds in warm, relatively fresh submarine spring discharge along this stretch of coastline (Hunt and Rosa, 2009) lent further support to this interpretation.

Most recently, dye tracer and natural tracer geochemical methods were used to confirm the direct hydrological connection between the main LWRF effluent injection wells 3 and 4 with a patchwork of hundreds of small (~5 cm<sup>2</sup>) submarine springs located just offshore of Kahekili Beach and to quantify SGD and associated nutrient fluxes in the area (Glenn et al., 2012, 2013). Other significant findings of that study were that (1) the discharge of the submarine springs off Kahekili beach park consists primarily (64%) of injected LWRF effluent, with a mean travel time of roughly 14 months, and (2) a large (but temporally variable) portion of N in the injected effluent is removed during subsurface transit via microbial nitrate reduction prior to its discharge at the coast. In addition, a large (~674,000 m<sup>2</sup>) plume of anomalously warm seawater in the vicinity of submarine springs at Kahekili Beach Park was found using aerial thermal infrared imagery and associated with the warm discharging

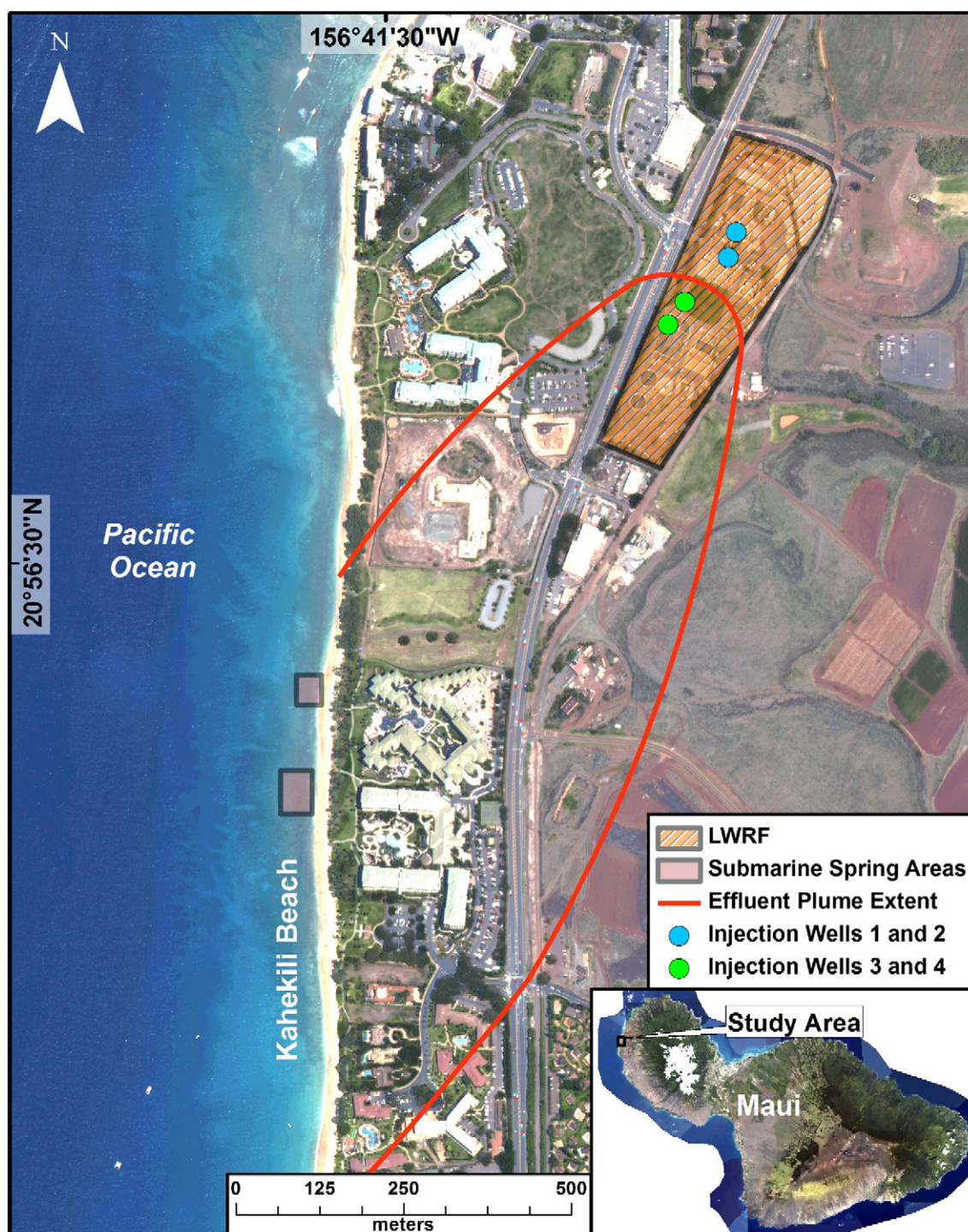


**Fig. 1.** Kā'anapali study area overview showing LWRF injections wells, Wells 3 and 4 effluent plume extent assessed by dye tracer in Glenn et al., 2013, and submarine spring area locations.

effluent (Glenn et al., 2012). Monthly monitoring of the submarine spring discharge by the State of Hawai'i Department of Health (HDOH) commenced in January 2012 and has since yielded new insights into the temporal variability of N concentrations in these waters.

### 3. Methods

#### 3.1. N species and $\delta^{15}\text{N}$ values of dissolved $\text{NO}_3^-$

To best assess the N species evolution between LWRF input and submarine spring output, we considered all available LWRF effluent and

submarine spring N species concentrations and  $\delta^{15}\text{N}$  values of dissolved  $\text{NO}_3^-$  available in both published literature and regulatory agency records; Table 1 provides a summary of data considered from these sources. Weekly LWRF N species concentration data collected for regulatory purposes ( $\text{NH}_4^+$ ,  $\text{NO}_2^- + \text{NO}_3^-$ , organic N, and total N) were obtained for the period of January 2008 through May 2013 along with monthly effluent Total Residual Chlorine (TRC) values from the period October 2011 through July 2014 from the County of Maui Wastewater Division. Discrete LWRF N species concentrations and  $\delta^{15}\text{N}$  of dissolved  $\text{NO}_3^-$  values are from Hunt and Rosa (2009) and Glenn et al. (2012). Submarine spring N species data is from Hunt and Rosa (2009);

**Table 1**

Summary of N species and  $\delta^{15}\text{N}$  of dissolved  $\text{NO}_3^-$  data collected from published works and regulatory agencies. The abbreviations LWRF and SS are used to denote LWRF effluent and submarine spring discharge sample types in this and all subsequent tables.

Sample information			Parameters reported				
Source	Type	Collection date(s)	Salinity	DO	TRC	N species	$\delta^{15}\text{N}$ of $\text{NO}_3^-$
LWRF Monitoring Program Hunt and Rosa (2009)	LWRF	1/2005 to 5/2013 <sup>1</sup>			X	X	
	LWRF	5/2008	X			X	X
	SS	5/2008	X			X	X
Swarzenski et al. (2012) Glenn et al. (2012)	SS	7/2010	X	X		X	
	LWRF	6/2011, 9/2011	X	X		X	X
	SS	6/2011, 9/2011, 1/2012	X			X	X
HDOH Monitoring Program	SS	2/2012 to 7/2014 <sup>2</sup>	X	X	X	X	

<sup>1</sup> Weekly sampling frequency.

<sup>2</sup> Monthly sampling frequency, with some months skipped.

Swarzenski et al. (2012); Glenn et al. (2012), and from monthly HDOH monitoring from January 2012 to July 2014. TRC is reported for several HDOH submarine spring samples. Submarine spring  $\delta^{15}\text{N}$  values of dissolved  $\text{NO}_3^-$  are from Hunt and Rosa (2009) and Glenn et al. (2012). Except for TRC, which is reported in units of mg/L, dissolved species concentrations are reported in units of  $\mu\text{M}$ .  $\delta^{15}\text{N}$  values of dissolved  $\text{NO}_3^-$  are reported in units of ‰ relative to AIR. LWRF and HDOH samples were analyzed in accordance with applicable USEPA procedures and can be assumed to have a maximum relative standard deviation of 10% for N species concentrations and 15% for TRC.

### 3.2. C species and $\delta^{13}\text{C}$ values of DIC

Water samples for C species analysis were split into 60 mL HDPE bottles from filtered LWRF effluent and submarine spring samples collected in June and September 2011 were kept chilled during transport before being frozen for storage prior to analysis. Samples were analyzed at the University of Hawai'i Water Resources Research Center Analytical Laboratory using a Shimadzu TOC-V Organic Carbon Analyzer. Samples were run separately for non-purgeable organic C (NPOC) and total C. Inorganic C values were obtained by subtracting NPOC from total C. Since the samples run were filtered through 0.45  $\mu\text{m}$  cellulose acetate filters, the values obtained for NPOC, total C and inorganic C are represented as DOC, total dissolved carbon (TDC), and DIC, respectively. The  $2\sigma$  values for analytical precision were 29  $\mu\text{M}$  for DOC, 60  $\mu\text{M}$  for TDC, and 67  $\mu\text{M}$  for DIC (propagated error as a derived quantity).

$\delta^{13}\text{C}$  of DIC samples were collected in September 2011 with minimal headspace in 20 mL borosilicate glass vials, crimp-sealed with aluminum caps and butyl rubber septa, and immediately poisoned via syringe with 0.5 mL of saturated  $\text{HgCl}_2$  solution. These samples were stored at room temperature to minimize the potential for leakage by the septa. Samples were analyzed at the University of Hawai'i Stable Isotope Biogeochemistry laboratory with a ThermoFinnigan Delta<sup>plus</sup>V mass spectrometer coupled to a GasBench II peripheral using the method of Salata et al., 2000. Results are reported in units of ‰ relative to PDB and normalized to the standards NBS-18 and NBS-19 using the accepted values of  $-5.04\text{‰}$  VPDB and  $1.95\text{‰}$  VPDB, respectively. The  $2\sigma$  value for analytical precision determined by duplicate sample analysis was 0.4‰.

### 3.3. Salinity unmixing of submarine spring discharge samples

For purposes of comparison with each other and with LWRF effluent, the highly variable salinities of the submarine spring samples considered in this study can be assumed to be a result of the dilution of the fresh component of the discharge with pore waters with normal ambient marine salinity. In order to normalize the DO, N species, and C species concentrations to the fresh water component of the submarine spring samples, the following equation was used to un-mix the ambient ocean water component of the samples:

$$C_1 = C_{\text{mix}} + (C_{\text{mix}} - C_2) \times (S_{\text{mix}} - S_1) / (S_2 - S_{\text{mix}}) \quad (1)$$

where  $C_1$  is the concentration of component 1, the hypothetical "source";  $C_2$  is the concentration of component 2, in this case seawater;  $C_{\text{mix}}$  is the concentration in the mixed sample being evaluated;  $S_1$  is the salinity of component 1, set equal to the suspected parent water;  $S_2$  is the salinity of component 2, in this case seawater; and  $S_{\text{mix}}$  is the salinity of the mixed sample being evaluated. In order to ensure consistency with previous studies of this system, we utilized the same seawater end member salinity and N species concentrations as Hunt and Rosa (2009) and Glenn et al. (2012), originally reported by Dollar and Andrews (1997). These samples were collected approximately 500 m offshore of the study area coastline over a time period of 6 months and as such represent the best seawater end member concentrations for these parameters available for this region. End member DOC, TDC, and DIC values were taken from the arithmetic mean values of these parameters for marine samples collected in September 2011 in support of Glenn et al. 2012. End member DO concentrations were taken from the arithmetic mean of the marine samples collected by HDOH in January 2012 and reported in Glenn et al. 2012. End member TRC was set at 0 based on the lack of natural free chlorine in the marine environment. The salinity of the treated wastewater effluent (here, the arithmetic mean salinity of the LWRF treated wastewater effluent samples measured in Glenn et al. 2012) was used as the hypothetical source salinity for ease of comparing unmixed submarine spring sample values with LWRF effluent sample values. The parameter values utilized for Eq. (1) are listed in Table 2.

## 4. Results

### 4.1. Wastewater effluent and submarine spring discharge data

Table 3 shows the results of LWRF and submarine spring samples analyzed for C species concentrations and (for September 2011 samples)  $\delta^{13}\text{C}$  values of DIC. Submarine spring samples ( $n = 5$ ) had DOC values ranging from 22 to 262  $\mu\text{M}$ , with an average value of 109  $\mu\text{M}$ , while LWRF effluent samples ( $n = 3$ ) had a higher average value (529  $\mu\text{M}$ ) over a smaller range (458–618  $\mu\text{M}$ ). In contrast, submarine spring DIC values (average = 2538  $\mu\text{M}$ , range 2106–2804  $\mu\text{M}$ ) were elevated

**Table 2**

End member parameters used in salinity unmixing of submarine spring discharge samples.

Parameter	Value	Reference
$S_1$	1.10	Glenn et al. (2012)
$S_2$	34.93	Dollar and Andrews (1997)
$C_2$ (DO)	225 $\mu\text{M}$	Glenn et al. (2012)
$C_2$ ( $\text{NH}_4^+$ )	0.19 $\mu\text{M}$	Dollar and Andrews (1997)
$C_2$ ( $\text{NO}_2^- + \text{NO}_3^-$ )	0.13 $\mu\text{M}$	Dollar and Andrews (1997)
$C_2$ (TN)	6.84 $\mu\text{M}$	Dollar and Andrews (1997)
$C_2$ (DON)	6.53 $\mu\text{M}$	Dollar and Andrews (1997)
$C_2$ (DOC)	176 $\mu\text{M}$	Glenn et al. (2012)
$C_2$ (TDC)	1815 $\mu\text{M}$	Glenn et al. (2012)
$C_2$ (DIC)	1631 $\mu\text{M}$	Glenn et al. (2012)
$C_2$ (TRC)	0 mg/L	N/A

**Table 3**

Submarine spring and LWRFC species and  $\delta^{13}\text{C}$  of DIC data. Mean values are indicated by bold font.

Sample information				Unmixed C species ( $\mu\text{M}$ )			
Sample date	Sample name	Type	Salinity	DOC	DIC	TDC	$\delta^{13}\text{C}$ of DIC (‰ VPDB)
6/2011	Seep 1 Piez 1	SS	2.0	114	2804	2918	
6/2011	Seep 2 Piez 1	SS	6.8	22	2778	2800	
6/2011	Seep 3 Piez 1	SS	5.0	61	2787	2848	
9/2011	Seep 3–2 Piez	SS	4.8	262	2106	2368	–11.1
9/2011	Seep 1–2 Piez	SS	2.9	85	2216	2301	–11.1
	<b>Mean</b>	<b>SS</b>	<b>4.3</b>	<b>109</b>	<b>2538</b>	<b>2647</b>	<b>–11.1</b>
6/2011	LWRF-1	LWRF	1.1	618	1925	2543	
9/2011	LWRF-EFF	LWRF	1.1	510	1432	1942	–11.2
9/2011	LWRF-R1	LWRF	1.1	458	1492	1950	–10.5
	<b>Mean</b>	<b>LWRF</b>	<b>1.1</b>	<b>529</b>	<b>1616</b>	<b>2145</b>	<b>–10.9</b>

with respect to the LWRF effluent values (average = 1616  $\mu\text{M}$ , range 1432–1925  $\mu\text{M}$ ). Submarine spring TDC values (average = 2647  $\mu\text{M}$ , range 2301–2918  $\mu\text{M}$ ) were generally higher than LWRF effluent TDC values (average 2171  $\mu\text{M}$ , range 1800–2542  $\mu\text{M}$ ) as well. With respect to the receiving ocean water (average DOC, DIC, and TDC = 176, 1631, and 1815  $\mu\text{M}$ , respectively), submarine spring samples were generally depleted in DOC and enriched in DIC and TDC.  $\delta^{13}\text{C}$  values of DIC was measured for two submarine spring samples as well as LWRF effluent and R-1 (irrigation quality effluent) samples collected in September 2011. The two submarine spring samples yielded identical  $\delta^{13}\text{C}$  values of DIC of –11.1‰ VPDB while the LWRF effluent and R-1 samples had similar  $\delta^{13}\text{C}$  values of DIC values of –11.2 and –10.5‰, respectively. Unmixed DO and N species results as well as  $\delta^{15}\text{N}$  values of dissolved  $\text{NO}_3^-$  for submarine spring and LWRF effluent samples reported in previous studies (excluding State of Hawaii Department of Health monitoring data, which are treated separately below) are presented in Table 4.

**Table 4**

Submarine spring and LWRF DO, N species, and  $\delta^{15}\text{N}$  of dissolved  $\text{NO}_3^-$  data from previous studies, excluding regulatory data. Mean values are indicated by bold font.

Sample information					Unmixed DO and N species ( $\mu\text{M}$ )					
Study	Sample date	Sample name	Type	Salinity	DO	TN	$\text{NO}_3^- + \text{NO}_2^-$	$\text{NH}_4^+$	DON	$\delta^{15}\text{N}$ of $\text{NO}_3^-$ (‰ VAIR)
Hunt and Rosa (2009)	5/2008	L1	SS	26.7			218.9	23.7		39.3
		L2	SS	29.7			228.5	104.5		39.7
		L5	SS	26.0			235.1			39.8
Swarzenski et al. (2012)	6/2010	T1-800-GW	SS	4.4	16.6	12.0	11.6	0.3	0.1	
		T2-900-GW	SS	1.7	55.6	49.7	39.1	0.1	10.5	
		T3-1000-GW	SS	2.7	30.6	55.1	44.1	0.1	10.9	
		T4-1100-GW	SS	1.5	19.4	52.7	42.7	0.1	9.8	
		T5-1200-GW	SS	2.8	24.4			0.1		
		T6-1300-GW	SS	2.5	15.6	54.6	43.9	0.1	10.6	
		T7-1400-GW	SS	2.9	24.7	57.4	44.2	0.1	13.2	
		T8-1500-GW	SS	2.9	26.9	55.5	44.0	0.0	11.5	
		T9-1600-GW	SS	3.0	25.6	53.9	44.2	0.2	9.5	
		T10-1700-GW	SS	3.3	35.3	53.3	44.4	0.1	8.9	
		T11-1800-GW	SS	3.4	20.9	32.7	30.1	2.4	0.2	
Glenn et al. (2012)	6/2011	Seep 1 Piez 1	SS	2.0		40.8	28.7	0.4	11.6	86.5
		Seep 1 Piez 2	SS	2.1		47.7	29.2	0.5	18.0	77.8
		Seep 2 Piez 1	SS	6.8		26.6	13.6	0.3	12.7	47.6
		Seep 3 Piez 1	SS	5.0		32.0	20.5	0.4	11.1	83.9
	9/2011	Seep 3–2 Piez	SS	4.8		125.2	8.5	0.5	116.2	93.1
		Seep 1–2 Piez	SS	2.9		122.1	13.0	0.5	108.6	83.0
	1/2012	North Seep A	SS	3.7	108.8	16.4	15.0	0.1	1.3	112.2
		North Seep B	SS	4.8	117.5	6.7	7.5	0.1		123.4
		North Seep C	SS	4.6	70.9	4.5	3.7	0.1	0.7	115.5
		South Seep A	SS	2.8	79.1	4.8	1.7	0.1	3.0	144.8
		South Seep B	SS	4.1	80.9	4.5	3.4	0.1	1.0	130.1
		South Seep C	SS	17.9	36.9	0.4	6.2	0.2		135.9
		<b>Mean</b>	<b>SS</b>	<b>6.7</b>	<b>46.5</b>	<b>41.3</b>	<b>48.9</b>	<b>5.4</b>	<b>18.5</b>	<b>90.2</b>
Hunt and Rosa (2009)	8-May	L12	LWRF	1.1		437.0	176.0	189.0	72.0	22.7
Glenn et al. (2012)	Jun-11	LWRF-1	LWRF	1.1	193.8	516.9	226.2	93.2	197.5	29.3
	Sep-11	LWRF-EFF	LWRF	1.1		457.9	282.9	11.1	163.9	30.9
		LWRF-R1	LWRF	1.1		432.6	256.6	19.0	157.0	31.5
		<b>Mean</b>	<b>LWRF</b>	<b>1.1</b>	<b>193.8</b>	<b>461.1</b>	<b>235.4</b>	<b>78.1</b>	<b>147.6</b>	<b>28.6</b>

#### 4.2. Long term monitoring of wastewater effluent N species and total residual chlorine

Table 5 shows summary statistics of average monthly LWRF effluent N species, injection flow rates, and TRC concentrations for the periods with available data from January 2005 to July 2014. Though all LWRF effluent N species concentrations show considerable variation,  $\text{NO}_3^- + \text{NO}_2^-$  (median 259.8  $\mu\text{M}$ ) typically constitutes the bulk of dissolved N in the injected effluent, with lesser proportions of  $\text{NH}_4^+$  (median 69.0  $\mu\text{M}$ ) and DON (median 96.3  $\mu\text{M}$ ). The large disparity between median and mean LWRF  $\text{NH}_4^+$  values reflects occasional plant upsets characterized by abnormally high  $\text{NH}_4^+$  values (Fig. 2) and consequently high proportion of TN as  $\text{NH}_4^+$ . These plant upsets or “ammonia spikes” are related to maintenance and personnel factors at LWRF (County of Maui Wastewater Division, personal communication). Injection wells 3 and 4, which have been shown to be hydrologically connected to the submarine springs via dye tracer test (Glenn et al., 2012, 2013), had a median effluent injection rate of 2.6 MGD which was 81.3% of the total the median effluent injection rate of 3.2 MGD during the period considered (Fig. 3). During the period of LWRF effluent chlorination (October 2011 through July 2014), effluent TRC concentrations varied widely with a median value of 1.4 mg/L (Fig. 5).

#### 4.3. Long term monitoring of submarine spring discharge N species and total residual chlorine

Table 6 shows summary statistics of average monthly submarine spring N species and unmixed TRC data for available periods from February 2012 to July 2014. All median submarine spring N species concentrations for this period were all over an order of magnitude less than those measured for the LWRF effluent reported above. The submarine spring N species distribution was dominated by  $\text{NO}_3^- + \text{NO}_2^-$  (median 57.0%) and DON (median 39.3%), containing relatively little  $\text{NH}_4^+$ .

**Table 5**

Summary statistics for monthly average LWRF N species, injection flow rate, and TRC.

Statistic	LWRF effluent N species 1/2005 through 5/2013 ( $\mu\text{M}$ )				LWRF injection flow rates 1/2011 through 7/2014 (MGD)		LWRF TRC 10/2011 through 7/2014 (mg/L)
	TN	$\text{NO}_3^- + \text{NO}_2^-$	$\text{NH}_4^+$	DON	Wells 3 + 4	Total	
Minimum	179.9	21.5	0.0	17.5	1.2	2.1	0.04
Median	459.3	259.8	69.0	96.3	2.6	3.2	1.42
Mean	466.0	270.2	104.6	97.7	2.5	3.3	1.90
Maximum	1380.9	554.5	1065.0	271.3	3.6	4.6	6.01
Standard deviation	172.4	110.2	144.7	34.3	0.5	0.6	1.47

(median 0.9%). Submarine spring unmixed TRC concentrations (Fig. 5) were also over an order of magnitude less than their LWRF effluent counterparts, with a median and mean value of 0.09 mg/L. The large disparities between the median and mean N species concentrations reflect a dramatic increase in submarine N species concentrations beginning in March 2013 (Fig. 4).

## 5. Discussion

### 5.1. Effluent plume biogeochemical reaction stoichiometry

N species transformations and attenuation within the STE are important modulators of SGD N flux. The presence and extent of these reactions can vary over small spatial and temporal scales and are governed by the complex interplay of hydrologic and geochemical forcing mechanisms. Previous studies examining N transformations in STEs have generally utilized a series of sampling points at multiple depths across the freshwater-seawater interface (e.g. Beck et al., 2007; Kroeger and Charette, 2008; Gonneea and Charette, 2014). In this study, however, we are limited to considering samples collected at the input (LWRF effluent) and output (submarine spring discharge) of the STE under investigation, complicating the evaluation of N transformations occurring within the effluent plume. In order to facilitate this evaluation, we consider the effluent plume as a closed system after accounting for seawater dilution of the submarine spring discharge via salinity unmixing as described above. LWRF effluent species constitute the inputs, while submarine spring discharge species represent the outputs.

The samples used to calculate the mean and standard deviations for submarine spring DOC, DIC, TDC, TN,  $\text{NO}_3^- + \text{NO}_2^-$ ,  $\text{NH}_4^+$ , and DON concentrations are from June 2011 and September 2011 ( $n = 5$ , Tables 2 and 3). Mean and standard deviation values for these species concentrations in LWRF effluent were calculated from June and September 2011 samples ( $n = 3$ ; Tables 3 and 4). DO mean and standard deviation values were calculated using the June 2010 measurements of Swarzenski et al. (2012) and January 2012 HDOH measurements of Glenn et al. (2012) ( $n = 17$ , Table 3). LWRF effluent mean DO was represented by a single measurement taken in June 2011 ( $n = 1$ ). From these data, Table 7 and Fig. 6 provide a summary of the difference in unmixed concentrations for DO as well as C and N species between the LWRF effluent and submarine spring discharge samples.

Fig. 6 shows that submarine spring discharge is enriched in DIC and TDC relative to the LWRF effluent, but depleted in all the other species considered (DO, DOC, TN,  $\text{NO}_3^- + \text{NO}_2^-$ ,  $\text{NH}_4^+$ , and DON). Although various N speciation and other biogeochemical reactions are likely occurring simultaneously within the effluent plume, for quantitative evaluation we consider them here as occurring separately in a stepwise fashion. We first consider a typical set of reactions (Table 8) observed in both natural systems (e.g. Kendall, 1998) and wastewater treatment plants (e.g. Henze et al., 2002). The ammonification of DON to  $\text{NH}_4^+$  is followed by the oxidation of  $\text{NH}_4^+$  to  $\text{NO}_3^-$  and the subsequent reduction of  $\text{NO}_3^-$  to  $\text{N}_2$  gas, utilizing DOC as an electron donor (heterotrophic denitrification).  $\text{NO}_3^- + \text{NO}_2^-$  is considered as  $\text{NO}_3^-$  for the purposes of the denitrification reaction, since  $\text{NO}_2^-$  represents an intermediate step in the process. Table 8 shows the theoretical progress of this set of reactions starting with LWRF species compositions and utilizing the actual

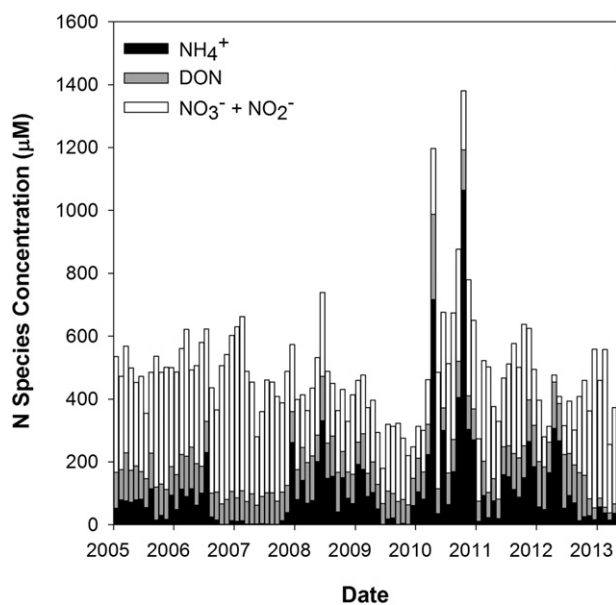


Fig. 2. LWRF effluent monthly average N species concentrations from January 2005 to May 2013. Note that the anomalously high TN values are generally associated with high  $\text{NH}_4^+$  concentrations.

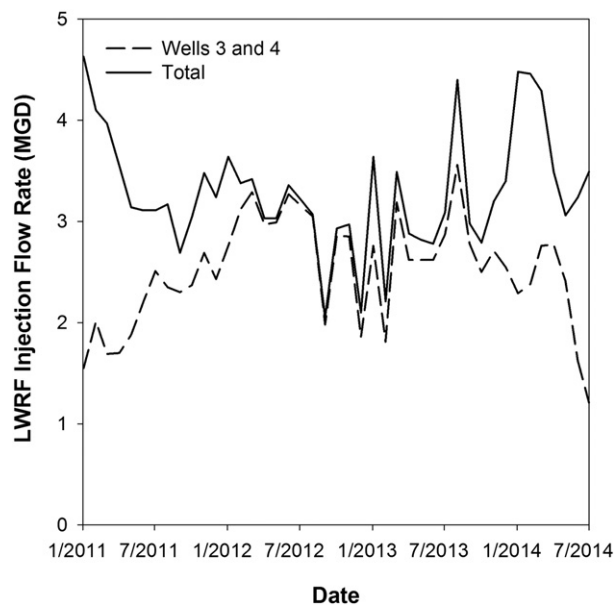


Fig. 3. Total LWRF injection rate shown with injection rate for wells 3 and 4. Wells 3 and 4 have a proven hydrologic connection to the submarine springs and receive the majority of LWRF effluent flow. Values are monthly averages.

**Table 6**  
Summary statistics for monthly average submarine spring N species and unmixed TRC.

Statistic	Submarine spring N species 2/2012 through 7/2014 ( $\mu\text{M}$ )				Submarine spring unmixed TRC 2/2012 through 7/2014 (mg/L)
	TN	$\text{NO}_3^- + \text{NO}_2^-$	$\text{NH}_4^+$	DON	
Minimum	3.6	0.1	0.0	3.1	0.05
Median	22.1	12.6	0.2	8.7	0.09
Mean	93.3	61.9	0.4	35.5	0.09
Maximum	387.8	251.6	2.2	179.6	0.17
Standard deviation	121.6	78.0	0.4	48.9	0.03

differences observed in species concentrations as the quantity of available reactant where applicable.

Table 8 shows that utilizing the differences between LWRF and submarine spring DON, DO, and  $\text{NO}_3^- + \text{NO}_2^-$  as limiting reagents for ammonification, nitrification, and heterotrophic denitrification, respectively, predicts the submarine spring DO concentration to within one standard deviation of its measured mean concentration (cf. Table 6). Predicted DIC and TDC concentrations are, however, 533 and 502  $\mu\text{M}$  lower than the actual submarine spring measured mean concentrations, but this discrepancy is very likely due to the dissolution of carbonate minerals to produce DIC within the alluvium along the LWRF-submarine spring flow path, as discussed below (Section 5.2). There also exists a large difference between the predicted submarine spring discharge  $\text{NH}_4^+$  concentration of 89  $\mu\text{M}$  and the observed mean  $\text{NH}_4^+$  concentration of 0  $\mu\text{M}$ . This difference results from the LWRF effluent having insufficient DO available to facilitate the complete nitrification of the 162  $\mu\text{M}$  of  $\text{NH}_4^+$  modeled to be present following the ammonification step in Table 7. There are several potential explanations for this discrepancy. First, it remains possible for  $\text{NH}_4^+$  to be partially oxidized to  $\text{NO}_2^-$  (utilizing 1.5 mol of DO per mole  $\text{NH}_4^+$  converted) or  $\text{N}_2\text{O}$  (utilizing 1 mol of DO per mole  $\text{NH}_4^+$  converted). Partial oxidation of  $\text{NH}_4^+$  to  $\text{NO}_2^-$  instead of  $\text{NO}_3^-$  would result in a slightly lowered predicted submarine spring  $\text{NH}_4^+$  concentration of 64  $\mu\text{M}$ , while partial oxidation of  $\text{NH}_4^+$  to  $\text{N}_2\text{O}$  instead of  $\text{NO}_3^-$  would result in changes to the predicted submarine spring species concentrations for DOC, DIC, TN, and  $\text{NH}_4^+$  to 232, 1914, 82, and 13  $\mu\text{M}$ , respectively. While bringing the predicted N species values closer to the observed, these reactions would result in

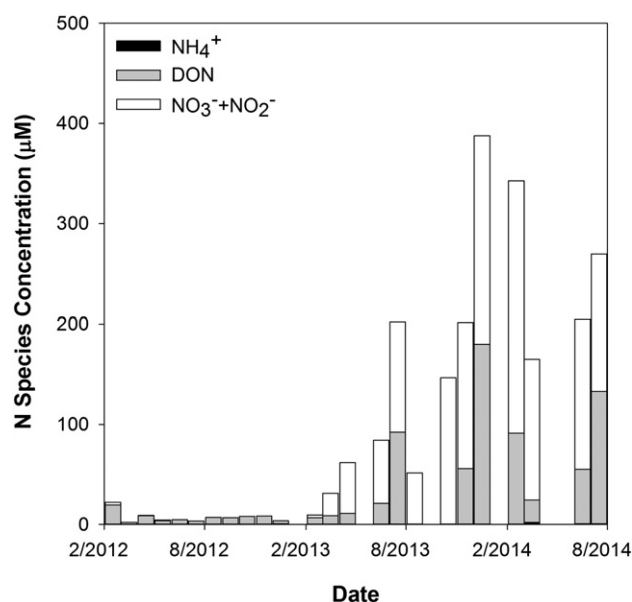


**Fig. 4.** Monthly average submarine spring N species concentrations from February 2012 to July 2014. TN values began to increase dramatically in March 2013.

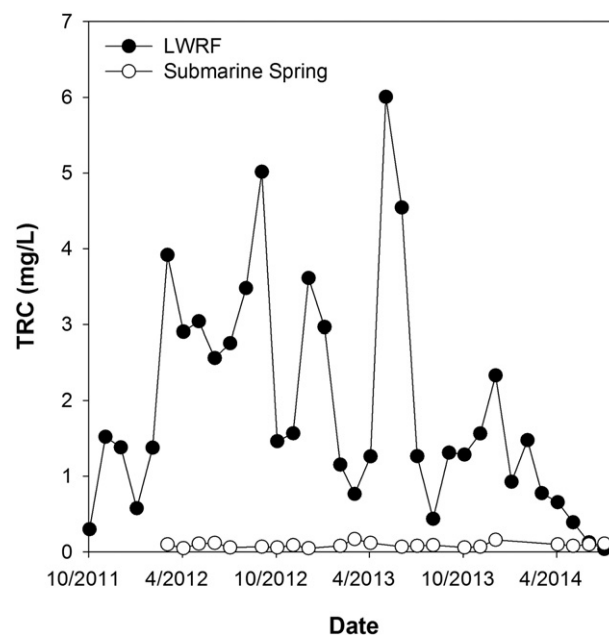


**Fig. 5.** LWRF and submarine spring TRC concentrations from the start of effluent chlorination at LWRF in October 2011 through July 2014. LWRF effluent chlorination was commenced in October 2011 and ceased in May 2014 after UV disinfection facilities were approved for use.

predicted C species values even farther from observed. A second and more likely explanation is that the Table 8 calculations overlook anaerobic ammonia oxidation, or anammox, which is the conversion of  $\text{NO}_2^-$  and  $\text{NH}_4^+$  to  $\text{N}_2$  gas and  $\text{H}_2\text{O}$  under anaerobic conditions. This reaction, first reported in wastewater systems (Mulder et al., 1995; Kuenen, 2008), has been integrated into engineered wastewater treatments and has also since been reported from a wide variety of natural oxygen-poor environments (e.g. Kuypers et al., 2005; Rich et al., 2008; Santoro, 2010; Terada et al., 2011; Zhu et al., 2013). Fresh groundwater environments in particular were identified by Sonthiphand et al. (2014) as ideal locations to study N-loss via anammox. The potential

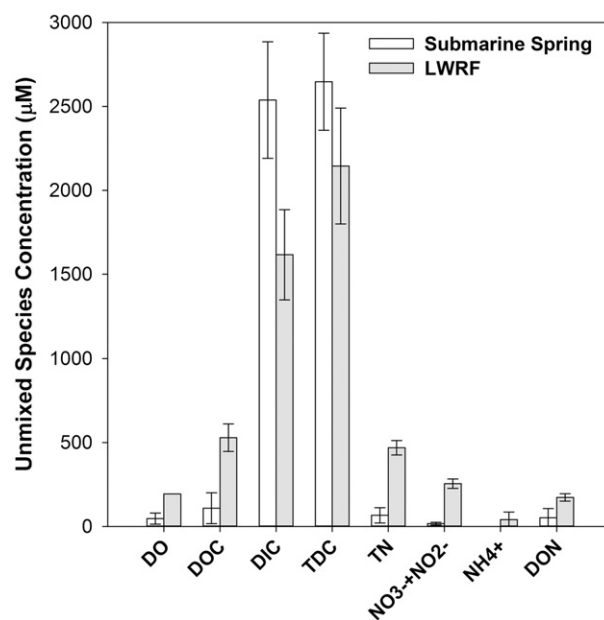


**Fig. 6.** Graphical representation of changes in unmixed DO, N species, and C species between LWRF effluent and submarine spring discharge. Error bars represent one standard deviation from the mean.

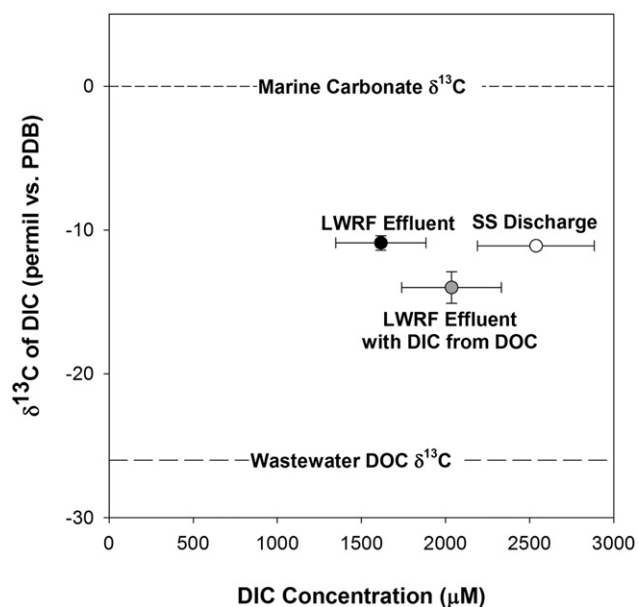


Fig. 7. The submarine spring discharge is augmented in DIC relative to the LWRF effluent via addition of DIC from consumption of DOC in heterotrophic processes (primarily denitrification) as well as dissolution of marine-derived carbonate within the aquifer. The data point for LWRF effluent with DIC from DOC is a hypothetical, calculated quantity. Error bars represent one standard deviation from the mean.

occurrence of anammox in the LWRF effluent plume was also suspected as based on observed nutrient and stable isotope parameters by Hunt and Rosa (2009).

The inclusion of anammox in the stepwise reactions (Table 9) allows us to more precisely account for the observed N species concentrations in the submarine spring effluent. Predicted DOC values and DIC values fall farther from the observed values (141 and  $-648 \mu\text{M}$ , respectively) than those predicted in Table 7 (31 and  $-533 \mu\text{M}$ , respectively), but these discrepancies can be improved by substituting, as above, the

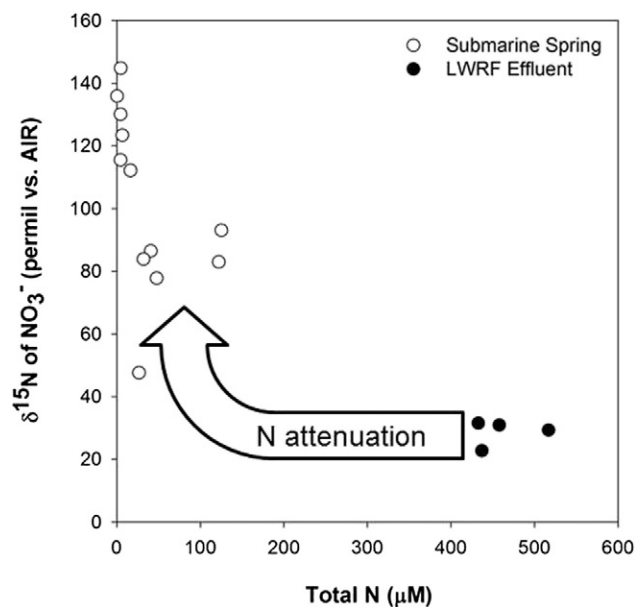


Fig. 8. Submarine spring discharge during the period these samples were taken (June 2011–January 2012, prior to the arrival of chlorinated effluent at the submarine springs) is characterized by low Total N concentrations and high  $\delta^{15}\text{N}$  of  $\text{NO}_3^-$  values relative to injected LWRF effluent. This is primarily the result of denitrification within the effluent plume, which preferentially reduces N-14 to  $\text{N}_2$  gas, leaving the remaining N enriched in N-15.

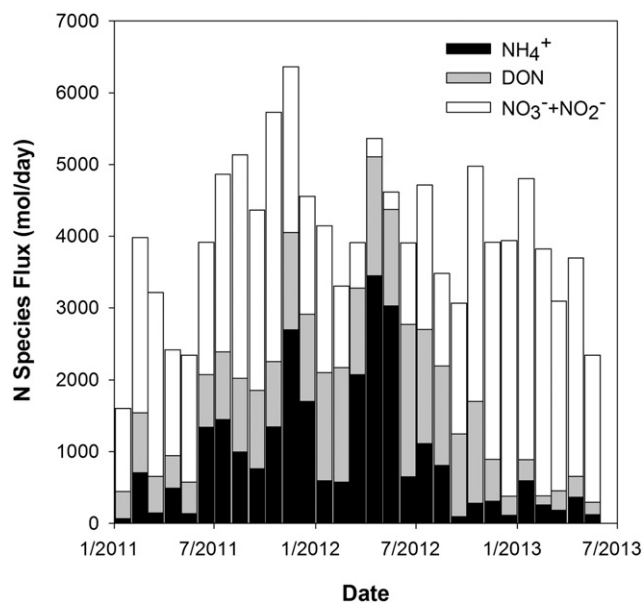


Fig. 9. LWRF effluent N-species fluxes from January 2011 to June 2013.

partial nitrification of  $\text{NH}_4^+$  to  $\text{NO}_2^-$  for the complete nitrification of  $\text{NH}_4^+$  to  $\text{NO}_3^-$ . This substitution results in predicted DOC and DIC values of 162 and  $1983 \mu\text{M}$ , respectively, moving the predicted DOC value to within one standard deviation of the mean of the observed values.

The stepwise stoichiometric analysis of hypothetical biogeochemical reactions occurring within the effluent plume can reasonably account for the observed concentrations of DO, C species, and N species in the submarine spring discharge within the constraints of this exercise. Nonetheless, many caveats still apply. It is important to note, for example, that the distributions of N and C species used here represent a small set of observations limited to June and September of 2011 and that both LWRF effluent and submarine spring discharge N and C species concentrations have been shown to exhibit considerable temporal variation (see Figs. 2 and 4 above). Due to the limited data available this analysis

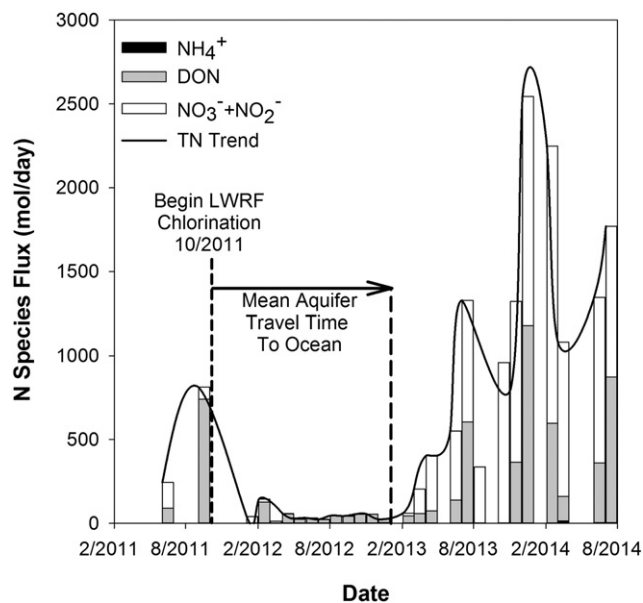


Fig. 10. Submarine spring N species flux from February 2011 to August 2014. Dates without bars indicate no available data. Note the marked increase in submarine spring TN flux to coastal ocean beginning about February 2013, roughly 14 months after the commencement of wastewater chlorination at the LWRF. 14 months corresponds to the mean transit time determined for the LWRF injection to submarine spring discharge flow path (Glenn et al., 2013).

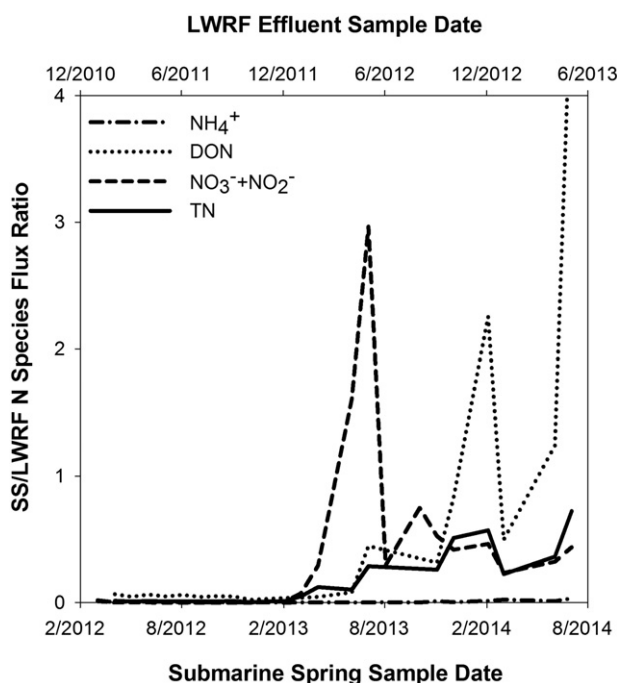


Fig. 11. Ratios obtained by dividing submarine spring N species flux by LWRF N species flux determined 14 months prior to the indicated date to account for travel time. The ratios of all N species fluxes except for  $\text{NH}_4^+$  increase dramatically after February 2013.

also did not consider variations in effluent injection rate, the estimated mean 14 month travel time from effluent injection to submarine spring discharge (Glenn et al., 2013), or the potential for admixture of groundwater from non-LWRF or marine sources (Glenn et al., 2012). The chemical equations used here to represent biogeochemical processes, while accurate enough for the large tolerances of this exercise, are simplified versions of more complex reactions (e.g. Zhou, 2007). Additionally, biogeochemical reactions not considered above that have been observed in subterranean estuaries, such as autotrophic denitrification (e.g. Kroeger

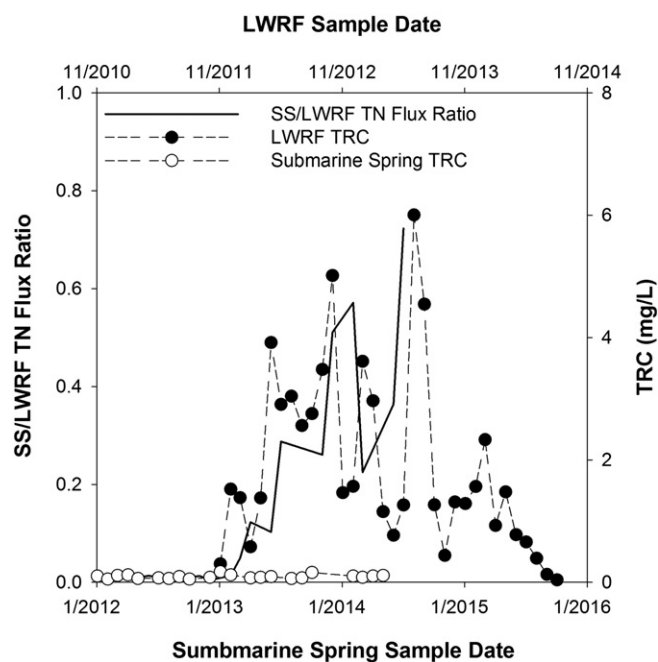


Fig. 12. The increase in SS/LWRF TN flux ratio closely parallels the increase in TRC concentration in the injected LWRF effluent when LWRF TN has been shifted forward 14 months to account for travel time.

and Charette, 2008), may also be occurring within the effluent plume and affecting final submarine spring species concentrations. Further measurement of LWRF and submarine spring C and N species as well as other dissolved species potentially involved in biogeochemical processes would be useful in characterizing the temporal variation in biogeochemical processes within the effluent plume and identifying additional biogeochemical reactions that may be occurring.

## 5.2. $\delta^{13}\text{C}$ values of DIC and $\delta^{15}\text{N}$ values of $\text{NO}_3^-$

$\delta^{13}\text{C}$  of DIC is a useful tracer of C sources in groundwater due to the large isotopic variations in potential source C reservoirs (Clark and Fritz, 1997). Within the LWRF effluent plume, the primary potential sources of DIC include both the DIC produced from heterotrophic consumption of DOC within the effluent during processing and after injection, as well as DIC liberated from the dissolution of carbonate rocks found in borings along portions of the effluent's flow path. The typical  $\delta^{13}\text{C}$  value of wastewater DOC is about  $-26.0\%$  VPDB (Griffith et al., 2009), while  $\delta^{13}\text{C}$  of marine limestone is typically near  $0\%$  VPDB (Clark and Fritz, 1997) and measured values of Pleistocene carbonates in Hawaii are similar (Fletcher et al., 2005). Since we have measured  $\delta^{13}\text{C}$  of DIC as well as DIC and DOC concentrations for LWRF effluent and submarine spring samples, we can utilize the following isotope mass balance to determine if the excess DIC observed in the submarine spring discharge has a  $\delta^{13}\text{C}$  of DIC value consistent with a marine limestone source:

$$[\text{DIC}]_{\text{LWRF}}\delta^{13}\text{C}_{\text{LWRF}} + [\text{DIC}]_{\text{DOC}}\delta^{13}\text{C}_{\text{DOC}} + [\text{DIC}]_{\text{EX}}\delta^{13}\text{C}_{\text{EX}} = [\text{DIC}]_{\text{SS}}\delta^{13}\text{C}_{\text{SS}} \quad (2)$$

where the variables above are defined as:

$[\text{DIC}]_{\text{LWRF}}$  = mean concentration of LWRF effluent DIC ( $1616 \mu\text{M}$ ).

$\delta^{13}\text{C}_{\text{LWRF}}$  = mean LWRF effluent  $\delta^{13}\text{C}$  of DIC ( $-10.9\%$  VPDB)

$[\text{DIC}]_{\text{DOC}}$  = concentration of DIC from DOC consumption ( $420 \mu\text{M}$ ,  $[\text{DOC}]_{\text{LWRF}} - [\text{DOC}]_{\text{SS}}$ ).

$\delta^{13}\text{C}_{\text{DOC}}$  = typical value of  $\delta^{13}\text{C}$  of DIC from wastewater DOC ( $-26.0\%$  VPDB)

$[\text{DIC}]_{\text{EX}}$  = concentration of excess DIC ( $502 \mu\text{M}$ ,  $[\text{DIC}]_{\text{SS}} - [\text{DIC}]_{\text{LWRF}} - [\text{DIC}]_{\text{DOC}}$ ).

$\delta^{13}\text{C}_{\text{EX}}$  = value of  $\delta^{13}\text{C}$  of excess DIC (unknown)

$[\text{DIC}]_{\text{SS}}$  = mean concentration of LWRF effluent DIC ( $2538 \mu\text{M}$ ).

$\delta^{13}\text{C}_{\text{SS}}$  = mean submarine spring  $\delta^{13}\text{C}$  of DIC ( $-11.1\%$  VPDB)

Solving Eq. (2) for  $\delta^{13}\text{C}_{\text{EX}}$  yields a value of  $\delta^{13}\text{C}$  of DIC value of  $0.7\%$  VPDB, which is consistent with a marine limestone source and especially close to the  $0.78\%$  VPDB value measured for a beachrock on the neighboring island of Molokai by Fletcher et al. (2005). If the equilibrium fractionation factor of  $9.0\%$  (Clark and Fritz, 1997) is applied to the conversion of the  $\text{CO}_2$  produced by the heterotrophic denitrification reaction to  $\text{HCO}_3^-$ , the  $\delta^{13}\text{C}_{\text{DOC}}$  value becomes  $-24.2\%$ . Substitution of this value into Eq. (2) yields a  $\delta^{13}\text{C}_{\text{EX}}$  value of  $-0.8\%$  VPDB, also well within the range of marine limestone sources. This simple sensitivity analysis of the isotope mass balance model strongly support our simplified assumption that dissolution of carbonate materials along the effluent plume's flow path is the source of the measured submarine spring DIC values in excess of those predicted by summation of DIC originally in the LWRF effluent and DIC produced by the consumption of DOC between LWRF effluent injection and submarine spring discharge. Fig. 7 shows a graphical representation of the evolution of DIC and  $\delta^{13}\text{C}$  of DIC values within the effluent plume.

The occurrence of temporally variable but extremely high  $\delta^{15}\text{N}$  of  $\text{NO}_3^-$  values in submarine spring discharge samples (mean  $90.2\%$  VAIR) was discussed at length in Glenn et al. 2012. It was determined that these high values, in conjunction with the drastic reduction in  $\text{NO}_3^- + \text{NO}_2^-$  concentrations along the LWRF-submarine spring flow path, were indicative of extensive, though temporally variable, denitrification of original LWRF  $\text{NO}_3^- + \text{NO}_2^-$  prior to submarine spring discharge. Although the stoichiometric analyses in Tables 8 and 9 of

**Table 7**

Calculated mean changes in unmixed DO, N species, and C species concentrations between injected LWRF effluent and submarine spring (SS) discharge.

		DO and C species ( $\mu\text{M}$ )				N species ( $\mu\text{M}$ )			
		DO	DOC	DIC	TDC	TN	$\text{NO}_3^- + \text{NO}_2^-$	$\text{NH}_4^+$	DON
SS	Mean	47	109	2538	2647	69	17	0	52
	Standard deviation	33	92	347	289	50	8	0	55
LWRF	Mean	194	529	1616	2145	469	255	41	173
	Standard deviation	NA	82	269	345	43	28	45	22
LWRF-SS $\Delta$	Mean	−147	−420	922	502	−400	−238	−41	−121
	Standard deviation	33	123	439	450	66	29	45	59

Section 5.1 above indicate that ammonification, nitrification, and potentially anammox play key roles in determining the ultimate N species composition of the submarine spring discharge, they also suggest that denitrification is responsible for the majority of N loss within the effluent plume. Significant N loss via denitrification has been frequently documented in subsurface wastewater plumes (e.g. Aravena and Robertson, 1998; Kroeger et al., 2006). This phenomena may be attributed to organic C in wastewater effluent fueling the heterotrophic consumption of  $\text{O}_2$  resulting in low  $\text{O}_2$  conditions favorable to denitrification. Fig. 8 provides an overview of the relationship of TN and  $\delta^{15}\text{N}$  values of  $\text{NO}_3^-$  in LWRF effluent and submarine spring samples. As explored below, future stable isotope measurements of  $\text{NO}_3^-$  as well as other N species in the LWRF effluent and submarine spring discharge will be useful in further understanding the dynamics of the various biogeochemical N transformations occurring within this effluent plume through time.

### 5.3. Temporal variation in effluent N fluxes vs. submarine spring discharge N fluxes

Comparison of LWRF effluent injection and submarine spring discharge N species fluxes provides a useful means for evaluating the dominant factors controlling effluent plume biogeochemistry. LWRF effluent injection N fluxes (Fig. 9), were calculated by multiplying mean monthly N species concentrations by mean monthly injection well 3 and 4 flows. Wells 1 and 2 flows were discounted due to their comprising a small percentage of total flow. Submarine spring N fluxes (Fig. 10) were calculated by multiplying the mean monthly salinity-unmixed N species concentrations by the single mean fresh SGD flux of 1.73 MGD determined for the submarine springs via radon mass balance (Glenn et al., 2013). These submarine spring N fluxes do not account for injected LWRF effluent entering the ocean via diffuse seepage at locations other than the submarine spring discharge locations shown in Fig. 1 and thus likely represent minimum N fluxes to the ocean from this source. Additionally, due to a lack of long-term SGD monitoring data, our calculated submarine spring N fluxes do not account for variations in SGD rate.

In order to directly compare input LWRF N species fluxes with output submarine spring N species fluxes on a temporally adjusted basis, we divided the submarine spring N species fluxes by the LWRF N species fluxes determined for 14 months prior (Fig. 11). This time shift accounts for the observed mean 14 month travel time between LWRF effluent injection and submarine spring discharge determined by Glenn et al.

2013. If LWRF effluent N species flux is the only control on submarine spring N species flux, these ratios should appear consistent over time. In reality, calculated SS/LWRF N species flux ratios remain relatively low and consistent through February 2013, after which date all N species ratios except for  $\text{NH}_4^+$  increase dramatically. This is indicative of a sudden alteration in the effluent plume to conditions much less favorable to N loss. The most parsimonious explanation is a reduction in the rates of DON ammonification as well as denitrification and/or anammox in the effluent plume. This explanation is consistent with results of stoichiometric modeling of aquifer biogeochemical reactions. Relatively constant near-zero values of the SS/LWRF flux ratio suggest that  $\text{NH}_4^+$  removal capabilities remained intact.

Chlorination of LWRF effluent prior to injection, which began in October 2011, roughly 16 months prior to the observed increase in SS/LWRF N species flux ratio, is consistent with a decrease in aquifer biogeochemical reactions. The purpose of wastewater chlorination is to kill waterborne pathogens (USEPA, 1999a). Chlorine gas ( $\text{Cl}_2$ ) reacts with water to produce the strongly oxidizing hypochlorous acid ( $\text{HOCl}$ ).  $\text{HOCl}$  may further dissociate to the hypochlorite ion ( $\text{OCl}^-$ ), another oxidizing compound. At the near neutral pH values measured in the LWRF effluent (Glenn et al., 2012),  $\text{HOCl}$ , the stronger oxidant, is the dominant aqueous species produced by the chlorination of water. We suggest that chlorination also adversely affected microbial activity in the aquifer, specifically that of microbes responsible for ammonification, nitrification, anammox, and denitrification within the effluent plume. Considering the mean aquifer transit time of approximately 14 months determined by fluorescein tracer dye testing (Glenn et al., 2012, 2013), the suppression of this microbial activity would thus explain the increase in the submarine spring discharge flux of TN, DON, and  $\text{NO}_3^- + \text{NO}_2^-$  beginning roughly 14 months after chlorination of injected LWRF effluent commenced. The lack of a simultaneous increase in submarine spring discharge  $\text{NH}_4^+$  flux during this same period implies an abiotic control on  $\text{NH}_4^+$  attenuation within the effluent plume. One possible abiotic  $\text{NH}_4^+$  attenuation mechanism may be the stepwise reaction of  $\text{HOCl}$  with  $\text{NH}_4^+$  to produce chloramines and ultimately  $\text{N}_2$  gas, a process known as “breakpoint chlorination” or “superchlorination” (Faust and Aly, 1998). We illustrate the past and possible future temporal correspondence between wastewater chlorination and its 14-month travel time delay on the resultant SS/LWRF TN flux ratio in Fig. 12. The increase in LWRF effluent TRC shifted 14 months forward closely parallels the increase in SS/LWRF TN flux ratio and attendant increase in TN discharged to the ocean from the submarine springs. The consistently low TRC values in submarine spring discharge suggest that the Cl

**Table 8**

Hypothetical stepwise changes in LWRF effluent composition through ammonification, nitrification, and denitrification processes based on reaction stoichiometry. The column heading ‘Limit’ refers to the species used as limiting reagent in the step considered in this and subsequent tables.

Step	Equation	Limit	DO	DOC	DIC	TDC	TN	$\text{NO}_3^- + \text{NO}_2^-$	$\text{NH}_4^+$	DON
Observed LWRF mean			194	529	1616	2145	469	255	41	173
Ammonification	$\text{RNH}_2 + \text{H}_2\text{O} + \text{H}^+ \rightarrow \text{ROH} + \text{NH}_4^+$	DON	194	529	1616	2145	469	255	162	52
Nitrification	$\text{NH}_4^+ + 2\text{O}_2 \rightarrow \text{NO}_3^- + \text{H}_2\text{O} + 2\text{H}^+$	DO	47	529	1616	2145	469	329	89	52
Denitrification	$4\text{NO}_3^- + 5\text{DOC} + 2\text{H}_2\text{O} \rightarrow 2\text{N}_2 + 4\text{HCO}_3^- + \text{CO}_2$	$\text{NO}_3^-$	47	140	2005	2145	158	17	89	52
Observed submarine spring mean			47	109	2538	2647	69	17	0	52
$\Delta$ (predicted-observed)			0	31	−533	−502	89	0	89	0

**Table 9**

Hypothetical stepwise changes in LWRF effluent composition through ammonification, nitrification, anammox, and denitrification processes.

Step	Equation	Limit	DO	DOC	DIC	TDC	TN	NO <sub>3</sub> <sup>-</sup> + NO <sub>2</sub> <sup>-</sup>	NH <sub>4</sub> <sup>+</sup>	DON
Observed LWRF mean			194	529	1616	2145	469	255	41	173
Ammonification	RNH <sub>2</sub> + H <sub>2</sub> O + H <sup>+</sup> → ROH + NH <sub>4</sub> <sup>+</sup>	DON	194	529	1616	2145	469	255	162	52
Nitrification	NH <sub>4</sub> <sup>+</sup> + 2O <sub>2</sub> → NO <sub>3</sub> <sup>-</sup> + H <sub>2</sub> O + 2H <sup>+</sup>	DO	47	529	1616	2145	469	329	89	52
Anammox	NH <sub>4</sub> <sup>+</sup> + NO <sub>2</sub> <sup>-</sup> → N <sub>2</sub> + 2 H <sub>2</sub> O	NH <sub>4</sub> <sup>+</sup>	47	529	1616	2145	292	240	0	52
Denitrification	4 NO <sub>3</sub> <sup>-</sup> + 5DOC + 2 H <sub>2</sub> O → 2 N <sub>2</sub> + 4HCO <sub>3</sub> <sup>-</sup> + CO <sub>2</sub>	NO <sub>3</sub> <sup>-</sup>	47	250	1895	2145	69	17	0	52
Observed submarine spring mean			47	109	2538	2647	69	17	0	52
Δ (predicted-observed)			0	141	-648	-502	0	0	0	0

demand within the effluent plume is sufficiently high to exhaust the disinfecting capabilities of the Cl<sub>2</sub> added to the LWRF effluent prior to its discharge.

Following HDOH approval of upgraded UV disinfection capabilities, LWRF effluent chlorination ended in May of 2014 (County of Maui Wastewater Division, Personal Communication). Unlike chlorination, UV disinfection does not result in the persistence of strong oxidants in the effluent plume following injection (USEPA, 1999b) and thus should not have an adverse effect on microbial populations within the effluent plume. Given the known residence time of the effluent plume in the aquifer, the submarine spring discharge should be largely free of previously chlorinated effluent by late 2015. We hypothesize that effluent plume microbial populations will recover, restoring effluent plume biogeochemical processes to those observed prior chlorination (see Section 5.1 above). Continued monitoring of submarine spring discharge will be vital to confirming that chlorination was indeed responsible for the increase in N flux from the submarine springs after February 2013 as well as understanding the speed and extent of the recovery process if observed.

## 6. Conclusions

This study has yielded two major conclusions. First, stepwise stoichiometric analysis using input and output N and C species concentrations, stable isotope values, and DO concentrations can provide significant insight into the presence and extent of various biogeochemical processes within a subsurface wastewater plume with a well-characterized flow path and transit time. This insight includes the findings that heterotrophic denitrification plays a key role in N attenuation within the effluent plume, and that anammox very likely also contributes to this net N attenuation as well. Second, chlorination of injected LWRF effluent beginning in October 2011 likely adversely affected microbial activity in the aquifer, resulting in an increase in observed submarine spring N flux offshore of Kahekili Beach beginning in February 2013. Continued monitoring of the submarine spring discharge can confirm that effluent chlorination caused increased N flux as well as provide understanding of the dynamics of a potential future restoration of the initially observed strongly N-attenuating biogeochemical conditions. These findings provide an accessible approach for workers seeking to understand and quantify biogeochemical processes within subsurface wastewater plumes with limited monitoring points and data as well as insight for regulators and wastewater treatment plant operators into potential consequences of chlorination of wastewater at facilities utilizing underground effluent injection.

## Acknowledgements

The authors would like to thank Scott Rollins with the Maui County Wastewater Division and Watson Okubo at the Hawaii State Department of Health for providing the historical data used in this research. We also thank Aly El-Kadi and Roger Babcock for providing technical expertise and reviewing earlier versions of this manuscript. The comments of two anonymous reviewers were helpful in improving this manuscript. This project has been funded by grants from the NSF Hawaii EPSCoR Program through the National Science Foundation under

award number EPS-0903833, the United States Environmental Protection Agency through the Hawaii State Department of Health (Grant No. INF20110364), the United States Army Engineer Research and Development Center (Grant No. INF20110342), and by a grant/cooperative agreement to Craig Glenn from the National Oceanic and Atmospheric Administration, Project R/HE-17, which is sponsored by the University of Hawaii Sea Grant College Program, SOEST, under Institutional Grant No. NA09OAR4170060 from NOAA Office of Sea Grant, Department of Commerce. The views expressed herein are those of the authors and do not necessarily reflect the views of NOAA or any of its subagencies. UNIH-SEAGRANT-JC-12-20. This publication is University of Hawaii School of Ocean and Earth Science and Technology Contribution Number 9651.

## References

- Aravena, R., Robertson, W.D., 1998. Use of multiple isotope tracers to evaluate denitrification in ground water: study of nitrate from a large-flux septic system plume. *Ground Water* 36 (6), 975–982.
- Beck, A.J., Tsukamoto, Y., Tovar-Sanchez, A., Huerta-Diaz, M., Bokuniewicz, H.J., Sanudo-Wilhelmy, S.A., 2007. Importance of geochemical transformations in determining submarine groundwater discharge-derived trace metal and nutrient fluxes. *Appl. Geochem.* 22, 477–490.
- Bricker, S., Longstaff, B., Dennison, W., Jones, A., Boicourt, K., Wicks, C., Woerner, J., 2007. Effects of Nutrient Enrichment in the Nation's Estuaries: A Decade of Change. NOAA Coastal Ocean Program Decision Analysis Series No. 26., National Centers for Coastal Ocean Science, Silver Spring, MD (328 p).
- Bruno, J.F., Selig, E.R., 2007. Regional decline of coral cover in the Indo-Pacific: timing, extent, and subregional comparisons. *PLoS One* 2 (8), e711. <http://dx.doi.org/10.1371/journal.pone.0000711>.
- Burnett, W.C., Bokuniewicz, H., Huettel, M., Moore, W.S., Taniguchi, M., 2003. Groundwater and porewater inputs to the coastal zone. *Biogeochemistry* 66, 3–33.
- Clark, I.D., Fritz, P., 1997. *Environmental Isotopes in Hydrology*. CRC Press, New York 328 p.
- Dailer, M.L., Knox, R.S., Smith, J.E., Napier, M., Smith, C.M., 2010. Using 15N values in algal tissue to map locations and potential sources of anthropogenic nutrient inputs on the island of Maui, Hawai'i, USA. *Mar. Pollut. Bull.* 60, 655–671.
- Dailer, M.L., Ramey, H.L., Saephan, S., Smith, C.M., 2012. Algal δ15N values detect a wastewater effluent plume in nearshore and offshore surface waters and three-dimensionally model the plume across a coral reef on Maui, Hawai'i, USA. *Mar. Pollut. Bull.* 64, 207–213.
- DeGeorges, A., Goreau, T.J., Reilly, B., 2010. Land-sourced pollution with an emphasis on domestic sewage: lessons from the Caribbean and implications for coastal development on Indian Ocean and Pacific coral reefs. *Sustainability* 2, 2919–2949.
- Dollar, S., Andrews, C., 1997. Algal Blooms off West Maui—Assessing Causal Linkages Between Land and the Coast Ocean. Final Report for National Oceanic and Atmospheric Administration Coastal Ocean Program Office and University of Hawai'i Sea Grant College Program. Honolulu, HI.
- Engott, J.A., and Vana, T.T., 2007. Effects of Agricultural Land-Use Changes and Rainfall on Ground-Water Recharge in Central and West Maui, Hawai'i, 1926–2004. U.S. Geological Survey Scientific Investigations Report 2007–5103, 56 p.
- Faust, S. D., and Aly, O. M., 1998. *Chemistry of Water Treatment*, Second edition. Boca Raton, Florida, CRC Press, 587 p.
- Fletcher III, C.H., Murray-Wallace, C.V., Glenn, C.R., Sherman, C.E., Popp, B.N., Hessler, A., 2005. Age and origin of late quaternary Eolianite, Kaiehu point (Moomomi), Molokai, Hawaii. *Coastal Research* 42, 97–112.
- Froelich, P.N., Klinkhammer, G.P., Bender, M.L., Luedtke, N., Heath, G.R., Cullen, D., Dauphin, P., Hammond, D., Hartman, B., Maynard, V., 1979. Early oxidation of organic matter in pelagic sediments of the eastern equatorial Atlantic: suboxic diagenesis. *Geochim. Cosmochim. Acta* 43, 1075–1090.
- Garrison, G.H., Glenn, C.R., McMurtry, G.M., 2003. Measurement of submarine groundwater discharge in Kahana Bay, O'ahu, Hawai'i. *Limnol. Oceanogr.* 48 (2), 920–928.
- Gingerich, S.B., Engott, J.A., 2012. Groundwater Availability in the Lahaina District, West Maui, Hawai'i. U.S. Geological Survey Scientific Investigations Report. 2012–5010 90 p.
- Glenn, C.R., Whittier, R.B., Dailer, M.L., Dulaiova, H., El-Kadi, A.I., Fackrell, J., Kelly, J.L., Waters, C.A., 2012. Lahaina Groundwater Tracer Study — Lahaina, Maui, Hawai'i.

- Final Interim Report Prepared for the State of Hawai'i Department of Health, the U.S. Environmental Protection Agency, and the U.S. Army Engineer Research and Development Center. <http://www.epa.gov/region9/water/groundwater/uic-pdfs/lahaina02/lahaina-final-interim-report.pdf>.
- Glenn, C.R., Whittier, R.B., Dailer, M.L., Dulaiova, H., El-Kadi, A.I., Fackrell, J., Kelly, J.L., Waters, C.A., Sevadjin, J., 2013. Lahaina Groundwater Tracer Study – Lahaina, Maui, Hawai'i. Final Report Prepared for the State of Hawai'i Department of Health, the U.S. Environmental Protection Agency, and the U.S. Army Engineer Research and Development Center. <http://www.epa.gov/region9/water/groundwater/uic-pdfs/lahaina02/lahaina-gw-tracer-study-final-report-june-2013.pdf>.
- Gonneea, M.E., Charette, M.A., 2014. Hydrologic controls on nutrient cycling in an unconfined coastal aquifer. *Environ. Sci. Technol.* 48, 14178–14185.
- Granger, J., Sigman, D.M., Lehmann, M.F., Torell, P.D., 2008. Nitrogen and oxygen fractionation during dissimilatory nitrate reduction by denitrifying bacteria. *Limnol. Oceanogr.* 53 (6), 2533–2545.
- Griffith, D.R., Barnes, R.T., Raymond, R.A., 2009. Inputs of fossil carbon from wastewater treatment plants to U.S. rivers and oceans. *Environ. Sci. Technol.* 43 (15), 5647–5651.
- Henze, M., Harremoës, P., Arvin, E., la Cour Jansen, J., 2002. *Wastewater Treatment: Biological and Chemical Processes*, third ed. Springer-Verlag, Berlin 433 p.
- Howarth, R.W., Marino, R., 2006. Nitrogen as the limiting nutrient for eutrophication in coastal marine ecosystems: evolving views over three decades. *Limnol. Oceanogr.* 51 (1(2)), 364–376.
- Hunt Jr., C.D., Rosa, S.N., 2009. A Multitracer Approach to Detecting Wastewater Plumes From Municipal Injection Wells in Near Shore Marine Waters at Kihei and Lahaina, Maui, Hawai'i. U.S. Geological Survey Scientific Investigations Report. 2009–5253 166 p.
- Kehew, A.E., 2000. *Applied Chemical Hydrogeology*. Upper Saddle River, New Jersey, Prentice Hall 368 p.
- Kendall, C., 1998. Tracing nitrogen sources and cycling in catchments. In: Kendall, C., McDonnell, J.J. (Eds.), *Catchment Hydrology*. Elsevier Science, Amsterdam, pp. 519–576.
- Kroeger, K.D., Charette, M.A., 2008. Nitrogen biogeochemistry of submarine groundwater discharge. *Limnol. Oceanogr.* 53 (3), 1025–1039.
- Kroeger, K.D., Cole, M.L., York, J.K., Valiela, I., 2006. Nitrogen loads to estuaries from waste water plumes: modeling and isotopic approaches. *Groundwater* 44 (2), 188–200.
- Kuenen, J.G., 2008. Anammox bacteria: from discovery to application. *Nat. Rev. Microbiol.* 6 (4), 320–326. <http://dx.doi.org/10.1038/nrmicro1857>.
- Kuyppers, M.M.M., Lavik, G., Woebken, D., Schmid, M., Fuchs, B.M., Amann, R., Jørgensen, B.B., and Jetten, M.S.M., 2005. Massive nitrogen loss from the Benguela upwelling system through anaerobic ammonium oxidation. *Proc. Natl. Acad. Sci. U. S. A.* v. 102: 6478–6483. [www.pnas.org/cgi/doi/10.1073/pnas.0502088102](http://www.pnas.org/cgi/doi/10.1073/pnas.0502088102).
- Kwon, E.Y., Kim, G., Primeau, F., Moore, W.S., Cho, H.M., DeVries, T., Sarmiento, J.L., Charette, M.A., Cho, Y.K., 2014. Global estimate of submarine groundwater discharge based on an observationally constrained radium isotope model. *Geophys. Res. Lett.* 41, 8438–8444. <http://dx.doi.org/10.1002/2014GL061574>.
- Laws, E.A., Brown, D., Peace, C., 2004. Coastal water quality in the Kihei and Lahaina districts of the island of Maui, Hawai'i Islands. Impacts from physical habitat and groundwater seepage: implications for water quality standards. *Int. J. Environ. Pollut.* 22, 531–547.
- Moore, W.S., 1999. The subterranean estuary: a reaction zone of ground water and sea water. *Mar. Chem.* 65, 111–125.
- Moore, W.S., 2006. The role of submarine groundwater discharge in coastal biogeochemistry. *J. Geochem. Explor.* 88 (1–3), 389–393.
- Mulder, A., van de Graaf, A.A., Robertson, L.A., Kuenen, J.G., 1995. Anaerobic ammonium oxidation discovered in a denitrifying fluidized-bed reactor. *FEMS Microbiol. Ecol.* 16, 177–183.
- Paerl, H.W., 1997. Coastal eutrophication and harmful algal blooms; importance of atmospheric deposition and groundwater as “new” nitrogen and other nutrient sources. *Limnol. Oceanogr.* 42 (5(2)), 1154–1165.
- Paytan, A., Shellenbarger, G.G., Street, J.H., Gonneea, M.E., Davis, K., Young, M.B., Moore, W.S., 2006. Submarine groundwater discharge: an important source of new inorganic nitrogen to coral reef ecosystems. *Limnology and Oceanography* 51, 343–348.
- Rich, J.J., Dale, O.R., Song, B., Ward, B.B., 2008. Anaerobic ammonium oxidation (anammox) in Chesapeake Bay sediments. *Microb. Ecol.* 55, 311–320.
- Salata, G.G., Roelke, L.A., Cifuentes, L.A., 2000. A rapid and precise method for measuring stable carbon isotope ratios of dissolved inorganic carbon. *Mar. Chem.* 69, 153–161.
- Santoro, 2010. Microbial nitrogen cycling at the saltwater-freshwater interface. *Hydrogeol. J.* 18, 187–202. <http://dx.doi.org/10.1007/s10040-009-0526-z>.
- Scavia, D., Bricker, S.B., 2006. Coastal eutrophication assessment in the United States. *Biogeochemistry* <http://dx.doi.org/10.1007/s10533-006-9011-0>.
- Sigman, D.M., Granger, J., DiFiore, P.J., Lehmann, M.M., Ho, R., Cane, G., van Geen, A., 2005. Coupled nitrogen and oxygen isotope measurements of nitrate along the eastern North Pacific margin. *Glob. Biogeochem. Cycles* 19, GB4022.
- Slopp, C.P., Van Cappellen, P., 2004. Nutrient inputs to the coastal ocean through submarine groundwater discharge: controls and potential impact. *Journal of Hydrology* 295, 64–86. <http://dx.doi.org/10.1016/j.jhydrol.2004.02.018>.
- Smith, S., Kimmerer, W.J., Laws, E.A., Brock, R.E., Walsh, T.W., 1981. Kaneohe Bay sewage diversion experiment: perspectives on ecosystem responses to nutritional perturbation. *Pac. Sci.* 35, 279–402.
- Soicher, A.J., 1996. Assessing Non-Point Pollutant Discharge to the Coastal Waters of West Maui, Hawai'i [M.S. thesis]. Honolulu, University of Hawai'i (98 p).
- Soicher, A.J., Peterson, F.L., 1997. Terrestrial nutrient and sediment fluxes to the coastal waters of West Maui, Hawai'i. *Pac. Sci.* 51, 221–232.
- Sonthiphand, P., Hall, M.W., Neufeld, J.D., 2014. Biogeography of anaerobic ammonia-oxidizing (anammox) bacteria. *Front. Microbiol.* 5 (399). <http://dx.doi.org/10.3389/fmicb.2014.00399>.
- Souza, W.R., 1981. Ground-Water Status Report, Lahaina District, Maui, Hawai'i, 1980. U.S. Geological Survey Open File Report 81–549 2 map sheets.
- Spiteri, C., Slopp, C.P., Charette, M.A., Tuncay, K., Meile, C., 2008. Flow and nutrient dynamics in a subterranean estuary (Waquoit Bay, MA, USA): field data and reactive transport modeling. *Geochim. Cosmochim. Acta* 72, 3398–3412.
- Stearns, H.T., MacDonald, G.A., 1942. *Geology and Groundwater Resources of the Island of Maui, Hawai'i*. Hawai'i (Territory) Division of Hydrography Bulletin. 7 (344 p).
- Stumm, W., Morgan, J.J., 1996. *Aquatic Chemistry*. Wiley, New York 1022 p.
- Swarzenski, P.W., Storlazzi, C.D., Presto, M.K., Gibbs, A.E., Smith, C.G., Dimova, N.T., Dailer, M.L., Logan, J.B., 2012. Nearshore Morphology, Benthic Structure, Hydrodynamics, and Coastal Groundwater Discharge Near Kahekili Beach Park, Maui, Hawai'i. U.S. Geological Survey Open File Report. 2012–1166 34 p.
- Szmant, A.M., 2002. Nutrient enrichment on coral reefs: is it a major cause of coral reef decline? *Estuaries* 25 (4b), 743–766.
- Terada, A., Zhou, S., Hosomi, M., 2011. Presence and detection of anaerobic ammonium-oxidizing (anammox) bacteria and appraisal of anammox processes for high-strength nitrogenous wastewater treatment: a review. *Clean Techn. Environ. Policy* 13, 759–781.
- Tetra Tech, Inc., 1993. Preliminary Assessment of Possible Anthropogenic Nutrient Sources in the Lahaina District of Maui – Final. Prepared for USEPA Region 9, the Hawai'i Department of Health, and the County of Maui July 1993, 116 p. plus appendices.
- Tetra Tech, Inc., 1994. Effluent Fate Study, Lahaina Wastewater Reclamation Facility, Maui, Hawai'i. Prepared for U.S. Environmental Protection Agency Region 9. 7 3p. plus appendices.
- United States Environmental Protection Agency, 1999a. Wastewater Technology Fact Sheet: Chlorine Disinfection. Office of Water, Washington D.C. 7 p.
- United States Environmental Protection Agency, 1999b. Wastewater Technology Fact Sheet: Ultraviolet Disinfection. Office of Water, Washington D.C. 7 p.
- Wilkinson, C., 2008. Status of Coral Reefs of the World: 2008. Global Coral Reef Monitoring Network and Reef and Rainforest Centre, Townsville, Australia 296 p.
- Williams, I., Sparks, R., 2008. Status and trends of benthic and fish communities around Maui. In: Vermeij, M. (Ed.), *Coral Reefs of Maui: Status, Stressors, and Suggestions*. Blurb, Inc., San Francisco, pp. 8–12.
- Zhou, S., 2007. Stoichiometry of biological nitrogen transformations in wetlands and other ecosystems. *Biotechnol. J.* 2, 497–507. <http://dx.doi.org/10.1002/biot.200600078>.
- Zhu, G., Wang, S., Wang, W., Wang, Y., Zhou, L., Jiang, B., Hubb, J.M.O.D.C., Risgaard-Petersen, N., Schwark, L., Peng, Y., Hefting, M.M., Jetten, M.S.M., Yin, C., 2013. Hotspots of anaerobic ammonium oxidation at land-freshwater interfaces. *Nat. Geosci.* 6, 103–107.